ADVANCED FUNCTIONAL MATERIALS
www.afm-journal.de

Antagonistic Two-Color Control of Polymer Network Formation

Arnau Marco, Marc Villabona, Tugce Nur Eren, Florian Feist, Gonzalo Guirado, Rosa M. Sebastián, Jordi Hernando, and Christopher Barner-Kowollik**

Offering high spatiotemporal resolution, dual wavelength-controlled soft matter network formation paves the way to advanced printing techniques with optimized performance. One of the most promising approaches is the antagonistic control of covalent bond-forming reactions with two colors of light, where photoexcitation with one wavelength induces a photochemical reaction, while irradiation with the other ceases it in the presence of the first color. Herein, we combine a photoactivatable diene precursor and a photoswitchable dienophile, establishing a dual-wavelength-gated cycloaddition reaction capable of controlling polymer crosslinking. Upon incorporation of the diene precursor into a methacrylate copolymer and the synthesis of a difunctional dienophile cross-linker, selective polymer network formation is promoted under sole UV illumination, while it can be efficiently suppressed with simultaneous redlight irradiation. Critically, the methodology is used for the preparation of solid polymer materials with antagonistic two-color control of their cross-linking status, ultimately allowing the fabrication of spatially patterned polymer films.

1. Introduction

The control of chemical reactions with light allows polymer network formation and manipulation remotely with spatiotemporal resolution,[1] an advantageous feature that is exploited in a variety of applications ranging from adhesive bonding[2] to polymer self-healing,[3] surface patterning,[4] and additive manufacturing.[5] Most of the light-induced network formation processes occur under irradiation with a single illumination source, which poses several limitations to the time and spatial accuracy with which they can be conducted.[6,7] For instance, photoactivated reagents can diffuse out of the irradiated region or survive longer than the photoexcitation time, thus precluding efficient spatiotemporal confinement of photopolymerizations. In addition, the spatial resolution with which reactive systems can be photoexcited with far-field optics is restricted by diffraction and, consequently, impedes light-controlled polymerization on the nanoscale. To overcome these hurdles, the use of two colors of light can effectively control polymer network formation,[6,7] which also provides additional advantages such as polymer post-modification,[8] multi-material preparation[9] and 4D printing.[10]

To perform dual wavelength network formation with enhanced spatiotemporal control, two main strategies are utilized as we have recently summarized in ref. [11] On the one hand, cooperative or synergistic photoactivation with two colors of light can be employed, where the absorption of photons of two different wavelengths by one[6,12] or two[13] reactive species is required to trigger liquid resist curing, thereby favoring polymer network formation in the overlapping volume element of the two irradiation beams. For instance, this behavior can be accomplished synergistically by using dual-color photoinitiators[6,12] or cooperatively with cross-linkers functionalized with two independently reactive chromophores.[13b] Although excellent results have been obtained with this approach,[6,12] polymerization/cross-linking outside of the two-color irradiated area can take place depending on the diffusivity and lifetime of the photoactivated species. To circumvent this limitation, antagonistic photochemical systems inspired by stimulated emission depletion (STED) microscopy have been devised, which make use of one excitation wavelength to induce polymerization and another to suppress it in an orthogonal manner.[7] Thus, by judiciously selecting the shapes of these two illumination beams, polymer network formation can be effectively confined spatially. Typically, the second color of light halts polymerization by annihilating the reactive excited state of a photoinitiator[14] or activating a photoresponsive inhibitor,[15]

A. Marco, M. Villabona, G. Guirado, R. M. Sebastián, J. Hernando
Departament de Química
Universitat Autònoma de Barcelona
Edifici C/n, Campus UAB, Cerdanyola del Vallès 08193, Spain
E-mail: jordi.hernando@uab.cat
T. N. Eren, F. Feist, C. Barner-Kowollik
Institute of Nanotechnology (INT)
Karlsruhe Institute of Technology (KIT)
Hermann-von-Helmholtz-Platz 1, 76344 Eggenstein-Leopoldshafen, Germany
E-mail: christopher.barnerkowollik@qut.edu.au
C. Barner-Kowollik
School of Chemistry and Physics
Centre for Materials Science
Queensland University of Technology (QUT)
2 George Street, Brisbane, QLD 4000, Australia

The ORCID identification number(s) for the author(s) of this article can be found under https://doi.org/10.1002/adfm.202415431

DOI: 10.1002/adfm.202415431

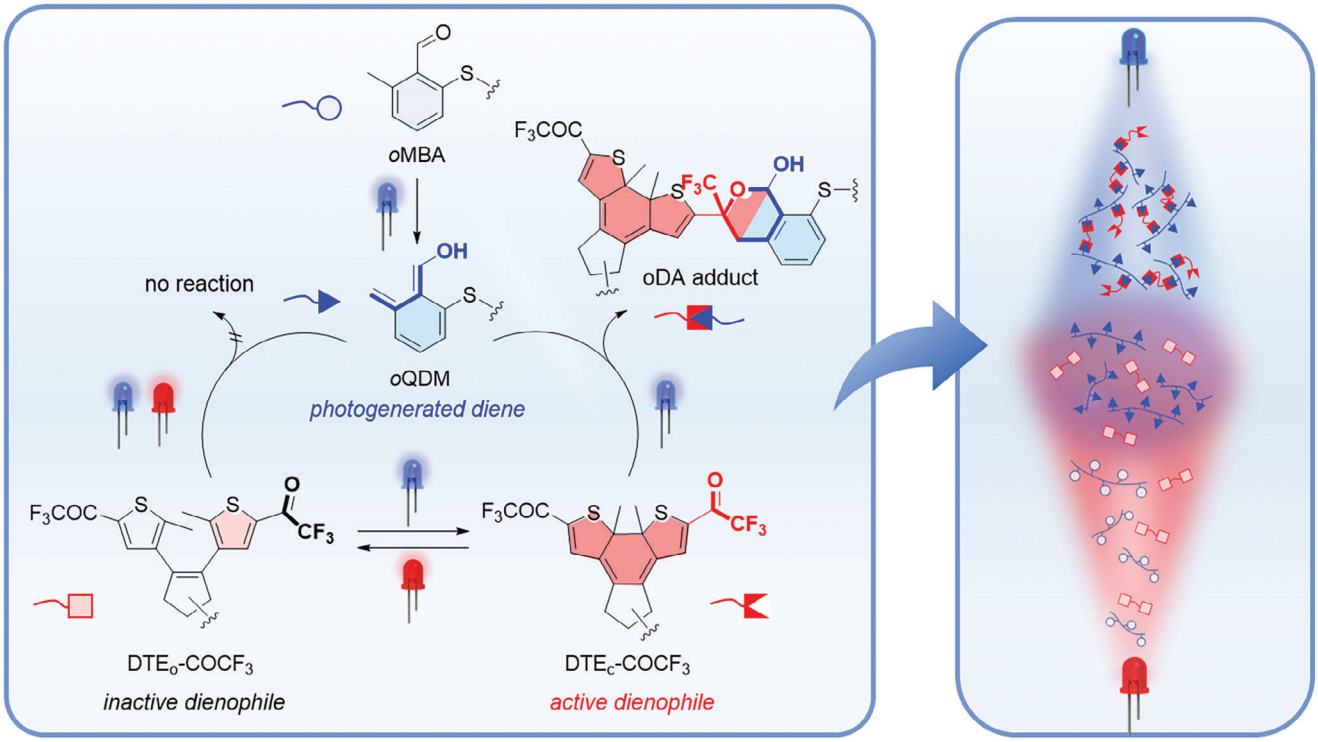

Scheme 1. Schematic representation of our antagonistic two-color photochemical reaction strategy to control polymer network formation by exploiting the light-modulated *oxo*-Diels-Alder reaction between photocaged dienes and photoswitchable dienophiles.

which however require very high excitation intensities and the incorporation of additional components to the formulation, respectively. Alternatively, the use of photoswitches has been proposed, which can toggle between active and inactive states for polymer curing under irradiation with two different excitation wavelengths.[16] However, despite its high promise, this strategy has been seldom exploited to date and – to fully unleash its potential— the development of novel antagonistic photoswitchable reactive systems is required.

Herein, we address this challenge by reporting an antagonistic two-color photochemical strategy based on photoswitchable motifs to control polymer network formation. With respect of previous studies, herein we propose a sophisticated dual color reaction scheme for polymer cross-linking: the use of two different bond-forming photoreactive entities to start and stop cross-linking reactions in an antagonistic fashion with two colors of light. To our knowledge, we follow an unprecedented approach, providing refined spatiotemporal resolution to polymer network formation, which we demonstrate to work not only in solution but also for the preparation of solid materials. We thus exploit a dual wavelength gated *oxo*-Diels-Alder cycloaddition (*o*DA) reaction recently described by us, which takes place under ambient conditions. Specifically, a photocaged *o*-methylbenzaldehyde precursor (*o*MBA) generates a transient *o*-quinodimethane diene (*o*QDM), which reacts with a trifluoromethyl ketone dienophile whose reactivity is reversibly altered by an appended dithienylethene photoswitch (DTE-$COCF_3$) (**Scheme 1**).[17] As a result, the *o*DA process is selectively triggered upon UV illumination by concomitantly generating the reactive *o*QDM and closed-state DTE-$COCF_3$ species (DTE_c-$COCF_3$), while it can be orthogonally suppressed with simultaneous red light irradiation by rendering the dienophile inactive in its open isomer form (DTE_o-$COCF_3$). We herein demonstrate that our antagonistic on-off photochemical system can be exploited for the two-color control of solid polymer network formation by reacting ***o*MBA**-pendant polymers (P*o*MBA) with difunctional DTE-$COCF_3$-based cross-linkers (**diDTE-$COCF_3$**) (Scheme 1). Notably, our approach can be extended to other polymers decorated with highly reactive photocaged diene precursors different from *o*MBA.

2. Results and Discussion

2.1. Synthesis and Photochemical Reactivity of Polymers and Cross-Linkers

To apply the two-color controlled *o*DA process to polymer network formation, the photoreactive **P*o*MBA** polymer and **diDTE-$COCF_3$** cross-linker were synthesized (**Figure 1a**). For **P*o*MBA** preparation, an *o*MBA-functionalized monomer was initially obtained by esterification between (hydroxyethyl)methacrylate and a carboxylic acid-terminated *o*-methylbenzaldehyde derivative previously reported by us[18] (***o*MBA-HEMA**, Scheme S1, Supporting Information). A mixture of ***o*MBA-HEMA** and methyl methacrylate (MMA) was subsequently subjected to free radical polymerization conditions to afford **P*o*MBA** as a methacrylate-based poly[MMA-*co*-***o*MBA-HEMA**] copolymer (Figure 1a; Scheme S1, Supporting Information). In a first step, a chain transfer agent was used to adjust the number average mass of the polymer formed close to 10 000 g mol^{-1}

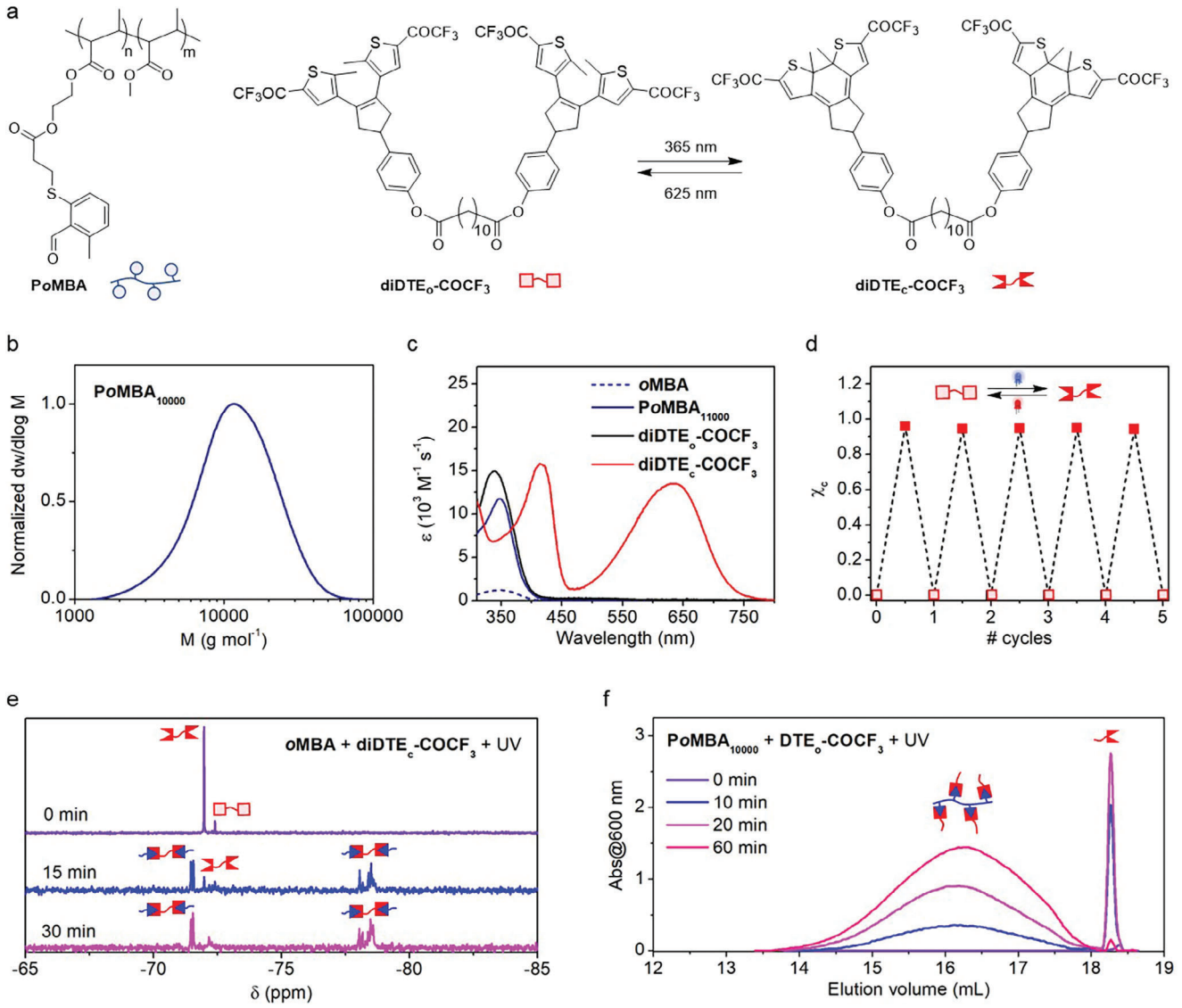

Figure 1. a) Structures of **PoMBA** and of the open and closed states of diDTE-COCF$_3$. b) SEC recorded molecular weight distribution of **PoMBA$_{10000}$**. c) UV–vis absorption spectra of ***o*MBA**, **PoMBA$_{10000}$**, **diDTE$_o$-COCF$_3$** and **diDTE$_c$-COCF$_3$** in toluene. d) Variation of the molar fraction of **diDTE$_c$-COCF$_3$** in toluene upon consecutive photoswitching cycles with UV (λ_{exc} = 365 nm) and visible (λ_{exc} = 625 nm) light irradiation. e) ^{19}F NMR spectra (282 MHz, toluene-d_8) of a reaction mixture of ***o*MBA** (c = 0.32 mM) and **diDTE$_c$-COCF$_3$** (c = 0.08 mM) subjected to UV irradiation (LED365 with $\lambda_{exc,max}$ = 365 nm, 1.17 mW cm^{-2}) under ambient conditions for 0, 15, and 30 min (refer to Section 4.1 in the Supporting Information for further details). f) SEC elugrams in THF of aliquots of a reaction mixture of **PoMBA$_{10000}$** (c = 0.83 mM) and **DTE$_o$-COCF$_3$** (c = 0.83 mM) in toluene-d_8 subjected to UV irradiation (LED365 with $\lambda_{exc,max}$ = 365 nm, 1.17 mW cm^{-2}) under ambient conditions for 0, 10, 20, and 60 min (refer to Section 4.2 in the Supporting Information for further details).

($\bar{M}_n$ = 10 400 g mol^{-1}, $Đ$ = 1.4), which should ensure sufficient solubility in organic solvents to allow analysis by size exclusion chromatography (SEC) even after substantial cross-linking (**PoMBA$_{10000}$**, Figure 1b; Figure S2 and Table S1, Supporting Information). The ***o*MBA-HEMA**:MMA monomer ratio in **PoMBA$_{10000}$** was determined to be 1:8, in line with the comonomer feed ratio used, and corresponds to around 9 *o*MBA pendant groups per chain (Figure S3 and Table S1, Supporting Information). The *o*MBA content was intentionally kept low to disfavor non-selective polymer cross-linking in subsequent experiments, which can take place by self-dimerization of two *o*QDM diene units photoproduced from *o*MBA.[8d] As a such process is promoted by high *o*MBA concentrations and UV irradiation intensities, reducing the ***o*MBA** monomer ratio in **PoMBA** should allow minimizing its contribution to polymer cross-linking relative to the desired *o*DA reaction with diDTE-COCF$_3$. The UV-vis absorption spectrum measured for **PoMBA$_{10000}$** in toluene solution was consistent with the presence of thioether-substituted *o*-methylbenzaldehyde pendant groups, which are known to exhibit a defined absorption band at $\lambda_{abs,max}$ ≈ 350 nm

(e.g., ***o*MBA** in Figure 1c, which is an *o*-methylbenzaldehyde monomer bearing a *n*-butylsulfanyl substituent).[17,18]

To achieve **P*o*MBA** cross-linking, the synthesis of the **diDTE-COCF$_3$** dimer was required due to the particular reactivity of its trifluoroacetyl moieties. Although each DTE-COCF$_3$ unit contains two equivalent lateral trifluoromethyl carbonyl dienophiles, only the first *o*DA photoligation between one of these groups and *o*MBA is favored in the closed isomer of the system.[17] The enhanced reactivity is caused by the electronic communication selectively established between the two initial electron-withdrawing trifluoromethyl ketones in DTE$_c$-COCF$_3$, which mutually reduces the electron density on their carbonyl groups and, therefore, critically enhances their dienophilic character. However, once the first of these groups undergoes *o*DA cycloaddition and transforms into a hemiketal species, this resonant activating effect is lost, which reduces the reactivity of the remaining trifluoromethyl ketone akin to that of the non-conjugated trifluoromethyl carbonyl moieties in DTE$_o$-COCF$_3$.[17] Thus, individual DTE-COCF$_3$ units cannot be used as cross-linkers of **P*o*MBA** operating via double *o*DA photoreaction, which led us to design a truly difunctional **diDTE-COCF$_3$** cross-linker.

To synthesize **diDTE-COCF$_3$**, we followed the strategy reported by Johnson and coworkers for the preparation of a different DTE dyad, which requires attaching a reactive phenol moiety to the central cyclopentene ring during the construction of the photoswitch scaffold.[19] As already reported by us,[17] we introduced the lateral trifluoromethyl ketone groups to the dithienylethene core by lithiation-mediated acylation of a dichlorinated DTE precursor, while dimerization was accomplished via double esterification of a dicarboxylic acid spacer with two of the phenol-DTE conjugates prepared (Scheme S2, Supporting Information). Thus, dodecandioic acid was selected as a linker due to two main reasons. First, we envisioned that its linear alkyl backbone provides sufficient conformational flexibility to favor the *o*DA photoligation reaction on both sides of the dimer. Second, it ensures large separation between the two individual DTE-COCF$_3$ units, a requirement to preserve their good photoswitching properties. In multiphotochromic compounds where DTE units are tethered through shorter spacers, the occurrence of excited state energy transfer processes detrimentally affects the efficiency of the second (and subsequent) ring-closing reactions and leads to incomplete photoconversion.[20] This drawback was prevented in **diDTE-COCF$_3$** due to the long C12 tether. Thus, when the UV-absorbing open-state **diDTE$_o$-COCF$_3$** obtained after synthesis was irradiated at λ_{exc} = 365 nm in toluene solution, nearly quantitative photoisomerization to the fully closed isomer **diDTE$_c$-COCF$_3$** was observed by sequential photocyclization of its two DTE$_c$-COCF$_3$ units (96% conversion in the photostationary state), which took place with high quantum yields ($\Phi_{o\text{-}c} \approx 0.38$ for the two ring-closing steps) (Figure 1c,d; Scheme S3, Figure S4, and Table S2, Supporting Information). Reverse photoisomerization from the blue-colored **diDTE$_c$-COCF$_3$** isomer to the initial colorless **diDTE$_o$-COCF$_3$** state was subsequently quantitatively promoted under red light irradiation (λ_{exc} = 625 nm, $\Phi_{c\text{-}o} \approx 0.011$ for the two photocycloreversion steps), allowing repetitive photoswitching of the compound with high efficiency and without apparent signs of photodegradation (Figure 1d).

As **P*o*MBA$_{10000}$** and **diDTE-COCF$_3$** entail the absorption spectra of monomeric *o*MBA and DTE-COCF$_3$ units, they could undergo *o*DA cycloaddition under similar UV irradiation conditions. Such a behavior was demonstrated by conducting separate model reactions between **P*o*MBA$_{10000}$** and **diDTE-COCF$_3$** with the corresponding DTE-COCF$_3$ and *o*MBA monomers in toluene, respectively. First, we investigated the photoreaction between the activated **diDTE$_c$-COCF$_3$** dienophile and an excess of ***o*MBA**, an *o*-methylbenzaldehyde monomer (Scheme S4, Figure 1e, and Figure S5, Supporting Information). When using ^{19}F NMR to monitor the evolution of this reaction mixture under irradiation with UV light (LED365 with $\lambda_{exc,max}$ = 365 nm, Figure S1, Supporting Information), the expected spectral changes confirming *o*DA photoligation were observed. Thus, the ^{19}F NMR signal of **diDTE$_c$-COCF$_3$** at δ = −71.97 ppm rapidly decreased and was totally consumed after 30 min, while a set of other resonances continuously grew in two clearly separated spectral regions: δ = −71.40– -71.60 ppm, and δ = −78.00– -78.70 ppm. Based on our previous study on the model *o*DA reaction between *o*MBA and DTE-COCF$_3$ monomers,[17] the latter can be attributed to the different stereoisomers of the cycloadduct resulting from the *o*DA process between the trifluoromethyl ketone dienophiles in **diDTE$_c$-COCF$_3$** and the *o*-quinodimethane diene photogenerated from ***o*MBA**, which generates asymmetric products with one reacted and one intact trifluoromethylcarbonyl groups for each DTE unit (Schemes S4, S5, Supporting Information). Consequently, this result indicates that the *o*DA reactivity of the trifluoroacetyl dienophiles of DTE-COCF$_3$ was preserved upon incorporation in the **diDTE-COCF$_3$** cross-linker. In addition, the cycloadducts formed maintained the photoswitching behavior of the initial diDTE-COCF$_3$ reagent, as they were initially produced in a blue-colored closed state that was reversibly transformed into the corresponding colorless open isomers under visible light irradiation (Schemes S4, S5 and Figure S5, Supporting Information).

Similar results were obtained when a mixture of **P*o*MBA$_{10000}$** and monomer **DTE$_c$-COCF$_3$** was irradiated at $\lambda_{exc,max}$ = 365 nm and investigated by ^{19}F NMR, though less defined, broader resonances were observed in this case for the cycloadducts formed due to the inherent heterogeneity of the reacting polymer scaffold (Scheme S6 and Figure S6, Supporting Information). Alternatively, the photoinduced *o*DA process between these compounds was monitored by SEC with selective absorption detection at λ_{abs} = 600 nm, for which we took advantage of the characteristic blue color of the closed isomer of both DTE-COCF$_3$ units and their cycloaddition product[17] (Figure 1f). Here, we started from a UV-absorbing mixture of **P*o*MBA$_{10000}$** and **DTE$_o$-COCF$_3$**, for which no relevant signal was detected in the initial SEC elugram. In contrast, two clear peaks were observed upon illumination with $\lambda_{exc,max}$ = 365 nm: 1) a narrow peak at an elution volume of *ca.* 18.3 mL, which is associated with the closed isomer **DTE$_c$-COCF$_3$** rapidly formed upon UV-induced photocyclization of the initial **DTE$_o$-COCF$_3$** reagent and progressively consumed via *o*DA reaction with the pendant *o*MBA groups of **P*o*MBA$_{10000}$**; and 2) a broad band ranging from *ca.* 14–18 mL of elution volume whose intensity increased with irradiation time, which corresponds to the polymer chains that become visible-light absorbing upon cycloadduct formation with **DTE$_c$-COCF$_3$** (Scheme S6, Supporting Information). Therefore, these results demonstrate that *o*MBA-DTE-COCF$_3$ *o*DA cycloaddition also efficiently occurs after incorporation of the *o*-methylbenzaldehyde precursors as side groups in the methacrylate copolymer backbone.

Table 1. Optimization of the experimental conditions for the two-color control of polymer cross-linking with **PoMBA$_{10000}$** and **diDTE-COCF$_3$**.

Experiment	Conditions[a]				$\bar{M}_n$ [g mol^{-1}]	$Đ$	diDTEo-COCF$_3$ *consumption* [%][c]	*Cross-linking efficacy* [%][d]	*Cross-linking inhibition* [%][e]
	$\lambda_{exc,max}$[b] [nm]	UV *power* [mW cm^{-2}]	$c_{PoMBA_{10000}}$ [mM]	$c_{diDTE_o-COCF_3}$ [mM]					
1A	365	2.91	4.2	4.2	22 500	27.9	98	58	–
1B	365 + 625	2.91	4.2	4.2	19 600	34.8	97	54	11
1C	365	2.91	4.2	0	14 200	1.7	–	20	–
2A	365	0.93	4.2	2.1	17 400	5.9	96	46	–
2B	365 + 625	0.93	4.2	2.1	14 000	2.0	62	28	69
2C	365	0.93	4.2	0	12 700	1.6	–	20	–
3A	365	0.93	4.2	1.0	17 000	3.0	100	42	–
3B	365 + 625	0.93	4.2	1.0	13 800	1.8	90	25	74
3C	365	0.93	4.2	0	12 700	1.6	–	19	–
4A	365	0.60	4.2	1.0	16 000	2.0	100	36	–
4B	365 + 625	0.60	4.2	1.0	12 900	1.5	56	13	100
4C	365	0.60	4.2	0	12 900	1.5	–	14	–
5A	365	0.60	1.0	0.25	13 100	1.6	100	27	–
5B	365 + 625	0.60	1.0	0.25	11 800	1.5	54	15	100
5C	365	0.60	1.0	0	12 500	1.5	–	20	–
6A	365	0.60	0.40	0.10	12 100	1.4	100	14	–
6B	365 + 625	0.60	0.40	0.10	11 400	1.3	33	5	100
6C	365	0.60		0	11 300	1.3	–	5	–

[a] Experiments conducted with irradiation of **PoMBA$_{10000}$** and **diDTE$_o$-COCF$_3$** mixtures in toluene solution (60 µL) for 60 min under ambient conditions; [b] UV irradiation at $\lambda_{exc,max}$ = 365 nm with variable power density indicated in the UV power column, and red irradiation at $\lambda_{exc,max}$ = 625 nm (464.7 mW cm^{-2}); [c] Estimated from the area of the peak in the SEC elugrams at ca. 18 mL elution volume, which corresponds to free **diDTE$_o$-COCF$_3$** and **diDTE$_c$-COCF$_3$** molecules; [d] Estimated by substracting the SEC signal of non-irradiated **PoMBA$_{10000}$** from the SEC elugrams of the photoreactions (see Figure 2b and the Supporting Information for further details); [e] Obtained by comparing the cross-linking efficicacies determined under UV or combined UV and red illumination of the **PoMBA$_{10000}$-diDTE$_c$-COCF$_3$** mixtures, after substracting the effect of the inherent self-cross-linking experienced by **PoMBA$_{10000}$** under UV irradiation (refer to the Supporting Information for further details).

2.2. Antagonistic Two-Color Control of Polymer Cross-Linking

Once we evidenced the *o*DA reactivity of **PoMBA$_{10000}$** and **diDTE-COCF$_3$** separately, we explored their combined use to accomplish antagonistic two-color control during polymer network formation, i.e., exploring if polymer cross-linking can be triggered under UV irradiation and efficiently inhibited upon simultaneous illumination with red light. To reach this goal, the effect of a variety of experimental parameters had to be considered owing to the complexity of our photochemical system, where several interdependent species can absorb UV and/or red radiation (**PoMBA$_{10000}$**, **diDTE$_o$-COCF$_3$**, **diDTE$_c$-COCF$_3$**, and the open and closed isomers of the cycloadduct product) and competing light-induced reactions might occur (e.g., **PoMBA$_{10000}$** cross-linking via *o*MBA self-dimerization). For simplicity, some of these parameters were preset in our photoreactivity study: the solvent, which we selected to be toluene to ensure high **PoMBA$_{10000}$** solubility and lengthen the lifetime of the reactive *o*QDM transient species photogenerated under UV illumination; the red light intensity used to halt polymer cross-linking, which we set to the maximum power density provided by two combined LED625 with $\lambda_{exc,max}$ = 625 nm (464.7 mW cm^{-2}); the reaction time (60 min), at which we targeted total conversion of the initial **diDTE-COCF$_3$** cross-linker; and the experimental geometry, where a thin liquid sample (60 µL placed in a closed glass flat-bottomed vial of 1 cm in diameter) was irradiated from below with $\lambda_{exc,max}$ = 365 nm and $\lambda_{exc,max}$ = 625 nm under strong air ventilation to prevent undesired heating (Figure S7, Supporting Information). In contrast, reagent concentration and UV irradiation intensity were adjusted in our light-controlled polymer cross-linking experiments to reach optimal dual-wavelength antagonistic behavior (**Table 1**).

Starting from a mixture of **PoMBA$_{10000}$** and **DTE$_o$-COCF$_3$**, three types of measurements were conducted for each set of conditions: A) irradiation at $\lambda_{exc,max}$ = 365 nm to promote polymer network formation via *o*DA reaction; B) combined irradiation at $\lambda_{exc,max}$ = 365 nm and $\lambda_{exc,max}$ = 625 nm to prevent *o*DA-based cross-linking by favoring **diDTE-COCF$_3$** to remain in its inactive open state; and C) irradiation at $\lambda_{exc,max}$ = 365 nm in the absence of **diDTE-COCF$_3$** to evaluate the extent of non-specific **PoMBA$_{10000}$** cross-linking via *o*MBA self-dimerization, an undesired process that should be minimized with respect to *o*DA-driven polymer cross-linking (**Figure 2a**; Figure S8, Supporting Information). For these experiments, the efficacy of light-induced polymer network formation was assessed by several parameters obtained from the SEC analysis of each photoreaction mixture after 60 min: $\bar{M}_n$, $Đ$ and the cross-linking percentage (Table 1). The latter was estimated by deconvoluting the SEC signal of the photoreacted polymer into two different components using the SEC elugram of the pristine initial polymer: a band for unreacted **PoMBA$_{10000}$**, and a band for the cross-linked polymer chains,

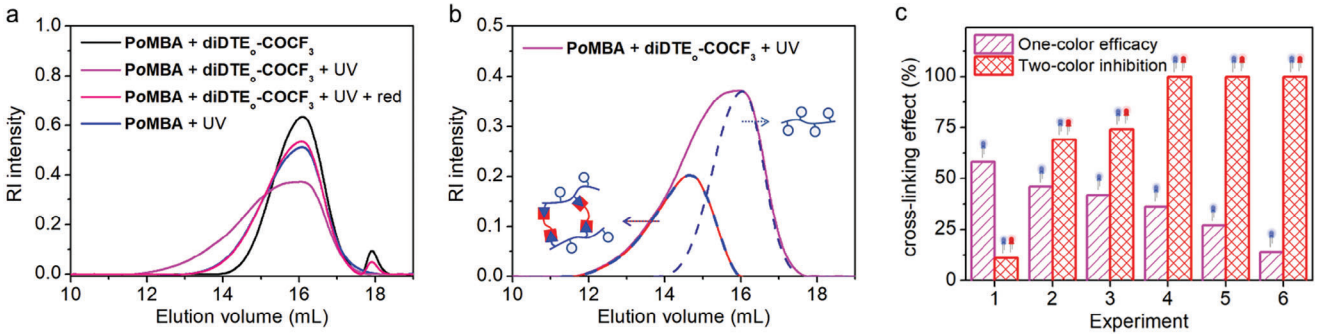

Figure 2. a) SEC elugrams of a non-irradiated **PoMBA$_{10000}$-diDTE$_o$-COCF$_3$** sample and of the photoreaction mixtures obtained for experiments 4A (**PoMBA$_{10000}$-diDTE$_o$-COCF$_3$** + UV), 4B (**PoMBA$_{10000}$-diDTE$_o$-COCF$_3$** + UV + red) and 4C (**PoMBA$_{10000}$** + UV) in Table 1. b) Deconvolution of the SEC elugram shown in a) for the UV-irradiated **PoMBA$_{10000}$** and **diDTE$_o$-COCF$_3$** photoreaction mixture, which was separated into two different components: a band for unreacted **PoMBA$_{10000}$**, and a signal for the cross-linked polymer chains. c) Percentages of cross-linking efficacy and cross-linking inhibition achieved under UV (one-color efficacy) and combined UV and red illumination (two-color inhibition), respectively. Data is shown for each of the sets of photoreaction experiments in Table 1 (experiments 1–6).

whose integrals were then put into relation to evaluate the cross-linking efficacy. Critically, in this calculation we assumed that no insoluble polymer network had been formed, and that the RI-responses of the cross-linked and non-cross-linked polymer are the same (Figure 2b,c; Figures S9–S11; refer to Section 5 in the Supporting Information for further details). In addition, the efficacy of cross-linking inhibition occurring via simultaneous two-color illumination was also determined by comparing the amount of cross-linking achieved for the irradiated **PoMBA$_{10000}$-diDTE$_c$-COCF$_3$** mixtures under one ($\lambda_{exc,max}$ = 365 nm) or dual-wavelength ($\lambda_{exc,max}$ = 365 nm and $\lambda_{exc,max}$ = 625 nm) excitation, for which we first corrected by the inherent self-cross-linking experienced by **PoMBA$_{10000}$** with UV light (Table 1 and Figure 2c; refer to section 5 in the Supporting Information for further details).

The initial experiments on our two-color antagonistic photochemical system were performed at high **PoMBA$_{10000}$** concentration (c = 4.2 mM) and cross-linker-polymer ratio (1:1) (experiments 1A-C in Table 1). As a result, high UV irradiation intensity was required to observe nearly complete **diDTE-COCF$_3$** consumption after illumination for 60 min (2.91 mW cm^{-2}), probably because the photogeneration of reactive *o*QDM species was decreased by the competitive light absorption between *o*MBA and DTE-COCF$_3$ units. Although these conditions led to high cross-linking efficacy under irradiation at $\lambda_{exc,max}$ = 365 nm (58%), low antagonistic modulation was accomplished upon two-color illumination (11% of cross-linking inhibition). It must be noted that the amplitude of the modulation effect is related to the composition of the photostationary state generated for the photoswitchable cross-linker under simultaneous UV and red-light irradiation: the more non-reactive **diDTE$_o$-COCF$_3$** and the less reactive **diDTE$_c$-COCF$_3$** molecules co-exist in this photostationary state, the lower the cross-linking reactivity should be. As the ring-closing quantum yield of **diDTE-COCF$_3$** upon UV irradiation is significantly larger than the ring-opening quantum yield of **diDTE-COCF$_3$** under red light ($\Phi_{o\text{-}c}/\Phi_{c\text{-}o}$ ≈35, Table S2, Supporting Information), a much higher red-light intensity than UV power would be needed to fully displace the photostationary state toward the non-reactive open isomer and, therefore, efficiently inhibit cross-linking. Even for the maximum red-light intensity that we could reach in our setup (464.7 mW cm^{-2} at $\lambda_{exc,max}$ = 625 nm), this condition could not be met for experiment 1B due to the high UV power used, which explains the minor antagonistic effect achieved.

In light of this result, subsequent experiments were conducted at the same **PoMBA$_{10000}$** concentration (c = 4.2 mM) but lower cross-linker-polymer ratios (from 1:2 to 1:4), thereby favoring the UV photoactivation of *o*MBA precursors over DTE-COCF$_3$ absorption (experiments 2A-C, 3A-C and 4A-C in Table 1). Consequently, the UV irradiation intensity could be decreased nearly 5-fold (from 2.91 to 0.60 mW cm^{-2}) without the need of increasing the reaction time to ensure full **diDTE-COCF$_3$** consumption. As expected, the red light-induced antagonistic effect was then critically enhanced and it became 100% efficient while maintaining a significant amount of cross-linking efficacy under one-color irradiation, i.e., true on-off control of *o*DA-driven polymer network formation could be achieved (experiments 4A-B in Table 1). This behavior is well illustrated by the SEC elugrams shown in Figure 2a for experiments 4A-C. On the one hand, a clear broadening in polymer weight distribution due to cross-linking was observed under UV irradiation of a **PoMBA$_{10000}$-diDTE-COCF$_3$** mixture (experiment 4A). On the other hand, simultaneous red-light illumination of this mixture (experiment 4B) essentially led to the same elugram as when a cross-linker free **PoMBA$_{10000}$** sample was UV irradiated (experiment 4C), thereby corroborating that *o*DA-induced polymer cross-linking was fully inhibited.

Despite the satisfactory results obtained, it must be noted that non-specific **PoMBA$_{10000}$** cross-linking via *o*MBA self-dimerization also occurred at the optimized conditions for the two-color control of the *o*DA photoligation process, although to a relatively low extent (14% for experiment 4C in Table 1). To further reduce the effect caused by the bimolecular reaction between two activated *o*QDM species, we performed two additional experiments at lower **PoMBA$_{10000}$** concentrations (to 0.40 mM) and the optimal cross-linker:polymer ratio and UV irradiation power already established (experiments 5A-C and 6A-C in Table 1). Non-specific **PoMBA$_{10000}$** cross-linking was essentially suppressed for the best of these experiments (5% for experiment 6C in Table 1), while preserving the two-color antagonistic behavior of the system. However, this result came at the expense of lower

diDTE-COCF$_3$-promoted cross-linking efficiencies. Thus, we did not use these low **PoMBA** concentration conditions for subsequent experiments, but rather adopted those established for experiments 4A-B in Table 1 as the optimal conditions to promote *o*DA-driven polymer cross-linking with two-color antagonistic control: $c_{\mathrm{PoMBA}_{10000}}$ = 4.2 mM, 1:0.25 molar **PoMBA$_{10000}$:diDTE-COCF$_3$** ratio, and 0.60 mW cm^{-2} of UV irradiance.

2.3. Antagonistic Two-Color Control of Solid Polymer Network Formation

None of the photoreaction experiments disclosed above led to the generation of solid polymer materials. Instead, the generated cross-linked polymer networks remained dissolved in toluene, and only when strongly increasing the UV irradiation times up to 120–180 min, the formation of a small amount of solid precipitate was observed (Figure S12, Supporting Information). To evidence the potential of our two-color antagonistic photochemical system for the preparation of solid polymer matrices, further experimental refining was conducted. In particular, we investigated whether solid polymer network formation could be favored by using higher molecular weight **PoMBA** as a substrate of the UV-induced *o*DA process, which should be more likely to generate insoluble materials upon cross-linking. After experimental optimization, the best results were obtained when using a 85:15 mixture of two different *o*-MBA-pendant polymers of low and high molecular weights: **PoMBA$_{8000}$** ($\bar{M}_n$ = 8000 g mol^{-1}, $Đ$ = 1.5, 11:1 MMA:***o*MBA-HEMA** monomer unit ratio) and **PoMBA$_{55000}$** ($\bar{M}_n$ = 54 600 g mol^{-1}, $Đ$ = 2.0, 10:1 MMA:***o*MBA-HEMA** monomer unit ratio) (Figure S2 and Table S1, Supporting Information).

When photoreacting such a mixture with **diDTE$_o$-COCF$_3$** at the optimal conditions established for pure **PoMBA$_{10000}$** (experiments 4A-C in Table 1), the desired two-color antagonistic behavior was accomplished (**Figure 3a**). Under illumination at $\lambda_{\mathrm{exc,max}}$ = 365 nm, the formation of a thin polymer film at the bottom of the irradiated vial was observed (≈10 µm in thickness, Figure S13a, Supporting Information), which could not be dissolved by subsequent treatment with an excess of toluene and exhibited the characteristic blueish color of the cycloadduct resulting from *o*DA reaction between *o*-MBA and DTE$_c$-COCF$_3$ units. Analysis by IR spectroscopy confirmed that the generated polymeric material was mainly composed of **PoMBA**, as expected for the cross-linked **PoMBA-diDTE-COCF$_3$** matrices (Figure S14, Supporting Information), whose thickness could be adjusted by varying the irradiation conditions (sample geometry, and UV irradiation power and time, Figure S13b–d, Supporting Information). In contrast, no solid polymer was obtained when the same starting **PoMBA$_{8000}$-PoMBA$_{55000}$-diDTE$_o$-COCF$_3$** sample was simultaneously irradiated with intense red light at $\lambda_{\mathrm{exc,max}}$ = 625 nm or when UV illumination was conducted in the sole presence of a **PoMBA$_{8000}$-PoMBA$_{55000}$** mixture (Figure 3a). Therefore, solid polymer network formation was not produced by unspecific *o*-MBA self-dimerization, yet selectively through *o*-DA cycloaddition-induced cross-linking with **diDTE-COCF$_3$**, which could be macroscopically inhibited upon two-color irradiation. Interestingly, the polymer films thus prepared were found to be stable for several months under ambient conditions, thus evidencing the thermal and photochemical stability of the cross-linked matrices obtained by *o*-DA cycloaddition. Only when exposed to strong and long-term UV irradiation, the films eventually lost their characteristic blueish color by irreversible photobleaching of their dithienylethene cross-linkers, yet without resulting in material decomposition.

In light of these results, we finally applied the dual-wavelength gated *o*DA cycloaddition between **PoMBA** and **diDTE-COCF$_3$** to prepare spatially-patterned polymer films, i.e., to induce generalized cross-linked polymer network formation by irradiating the entire photoreactive sample with UV light while locally inhibiting *o*DA-promoted crosslinking by confined red illumination through a mask (Figure 3b). To do so, we slightly modified the experimental setup used and replaced the LED with $\lambda_{\mathrm{exc,max}}$ = 625 nm employed for cycloaddition inhibition by a collimated laser beam at λ_{exc} = 650 nm placed on top of the sample (Figure S15, Supporting Information). After irradiation, the solid films obtained were rinsed with toluene to remove both unreacted cross-linkers and polymers that could affect their subsequent characterization. As shown in Figure 3c, both millimeter- and centimeter-sized geometric patterns were created in polymer films, which can be directly identified by the naked eye due to the different colors of the cross-linked and non-cross-linked areas (images (i), (iii) and (v) in Figure 3c). While the distinctive blue color of the closed-state *o*DA cycloadducts was observed in the regions where UV-induced polymer network formation took place, the red-illuminated areas where the cross-linking *o*DA reaction between **PoMBA** and **diDTE-COCF$_3$** was suppressed did not show any coloration.

This conclusion was corroborated by two additional experiments. On the one hand, bright-field optical microscopy imaging revealed the lack of polymer material deposition on the regions patterned under red light irradiation (images (ii) and (iv) in Figure 3c). Importantly, the dimensions of these regions as determined by optical microscopy matched those of the mask apertures, thus revealing the good resolution of our photopatterning technique on the millimeter scale. On the other hand, we monitored the color changes produced upon sequential illumination of the entire samples with visible or UV radiation to further identify the regions of the films where polymer cross-linking had been inhibited (Figure 3d; Figure S16, Supporting Information). As the photochromic properties of the initial **diDTE-COCF$_3$** cross-linkers are preserved after *o*DA cycloaddition, the areas where solid polymer network had been formed underwent reversible photoswitching between blue-colored (upon UV irradiation) and colorless states (under illumination with red light or sunlight). In contrast, the patterned areas remained colorless at all times, clearly indicating that they do not contain the photoisomerizable *o*DA cycloadducts responsible for polymer network formation, further confirming the selective inhibition of cross-linking. Consequently, these results combined are a proof-of-concept demonstration of the capacity of our two-color photochemical system to spatially control polymer network formation in an antagonistic fashion.

3. Conclusion

We herein introduce an antagonistic photochemical approach to accomplish spatially-controlled polymer network formation

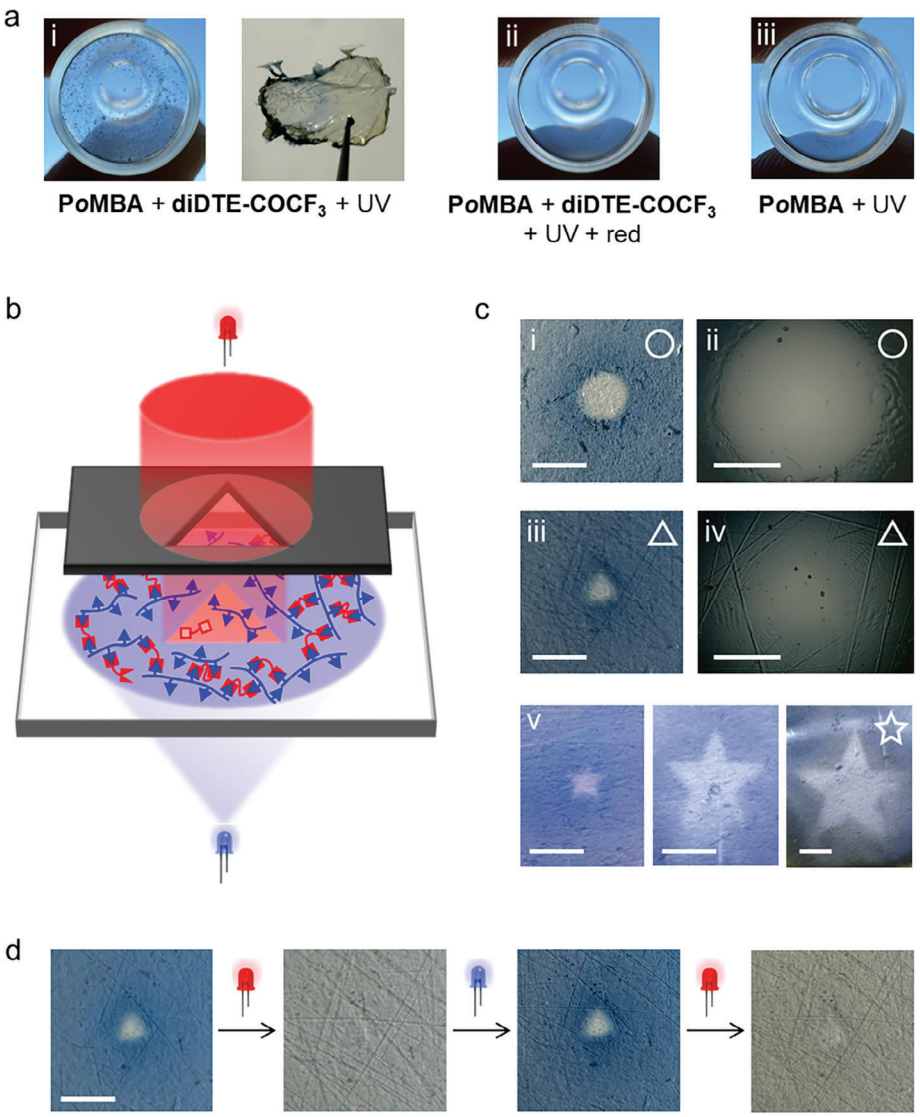

Figure 3. a) (i) Insoluble polymer thin film generated by irradiating a toluene solution of a 85:15 **PoMBA$_{8000}$**:**PoMBA$_{55000}$** mixture ($c_{\mathbf{PoMBA}}$ = 4.2 mM) and **diDTE$_o$-COCF$_3$** (c = 1.0 mM) at $\lambda_{exc,max}$ = 365 nm (0.60 mW cm^{-2}) for 60 min. No solid polymer material was formed when (ii) the same experiment was conducted with concomitant irradiation at $\lambda_{exc,max}$ = 625 nm (464.7 mW cm^{-2}), or (iii) an equivalent **diDTE$_o$-COCF$_3$**-free solution was treated with the same UV illumination conditions. b) Schematic representation of the experimental set-up used for the generation of patterned polymer films. c) (i, iii, v) Photographs (scale bar = 3.0 mm) and (ii, iv) bright-field optical microscopy images (scale bar = 1.0 mm) of the patterned polymer films obtained by irradiation of a toluene solution of a 85:15 **PoMBA$_{8000}$**:**PoMBA$_{55000}$** mixture ($c_{\mathbf{PoMBA}}$ = 4.2 mM) and **diDTE$_o$-COCF$_3$** (c = 1.0 mM) at $\lambda_{exc,max}$ = 365 nm (0.60 mW cm^{-2}) and λ_{exc} = 650 nm (509.3 mW cm^{-2}) for 60 min. Red light illumination was conducted through (i-ii) circle-, (iii-iv) triangle- and (v) star-shaped masks. d) Photographs of the triangle-patterned film upon sequential whole-field irradiation at $\lambda_{exc,max}$ = 625 nm and $\lambda_{exc,max}$ = 365 nm.

under irradiation with two colors of light. Our strategy takes advantage of a dual-wavelength gated *oxo*-Diels-Alder cycloaddition between a photogenerated diene and photoswitchable dienophile, which is promoted under UV irradiation and suppressed by red light illumination. By preparing a methacrylate copolymer decorated with the photocaged diene precursor and a difunctional photoswitchable dienophile, the cycloaddition reaction conditions were optimized to regulate polymer cross-linking under two-color irradiation, i.e., it was efficiently induced at λ_{exc} = 365 nm and could be halted upon concomitant illumination at λ_{exc} = 625 nm. Our antagonistic methodology was proven to enable two-color control of solid polymer network generation and—by shaping the red illumination beam—spatially-patterned polymer thin films were generated. Our results demonstrate the potential of combining photoactivatable and photoswitchable entities to reach refined on-off control of photocuring reactions, a strategy that provides a critical addition to the toolbox of dual-wavelength antagonistic approaches for polymer network formation with high spatiotemporal resolution.

Supporting Information

Supporting Information is available from the Wiley Online Library or from the author.

Acknowledgements

The study was supported by MICIU/AEI/10.13039/501100011033 and ERDF – "A way of making Europe" (PID2022-141293OB-I00) and Generalitat de Catalunya (2021 SGR 00064 and 2021 SGR 00052). M.V. and A. M. thank the Spanish Ministry for Education, Culture and Sports and the Generalitat de Catalunya for their predoctoral FPU and FI fellowships, respectively. J. H. is a Serra-Húnter Professor. C.B.-K. acknowledges funding by the Deutsche Forschungsgemeinschaft (DFG, German Research Foundation) under Germany's Excellence Strategy for the Excellence Cluster "3D Matter Made to Order" (EXC–2082/1 – 390761711), by the Carl Zeiss Foundation, and by the Helmholtz program "Materials Systems Engineering". The authors thank Alicia Schmidt (QUT/KIT) for her help with the graphical design of some of the figures.

Conflict of Interest

The authors declare no conflict of interest.

Data Availability Statement

The data that support the findings of this study are openly available in CORA.RDR at https://dataverse.csuc.cat.

Keywords

Antagonistic two-color photochemistry, Diels-Alder cycloaddition, Dithienylethenes, Light-controlled polymerization, *o*-Methoxybenzaldehydes

Received: August 21, 2024
Revised: December 19, 2024
Published online: January 2, 2025

[1] a) J. V. Crivello, E. Reichmanis, *Chem. Mater.* **2014**, *26*, 533; b) S. Chatani, C. J. Kloxin, C. N. Bowman, *Polym. Chem.* **2014**, *5*, 2187; c) E. Blasco, M. Wegener, C. Barner-Kowollik, *Adv. Mater.* **2017**, *29*, 1604005; d) S. P. Ihrig, F. Eisenreich, S. Hecht, *Chem. Commun.* **2019**, *55*, 4290; e) P. Lu, D. Ahn, R. Yunis, L. Delafresnaye, N. Corrigan, C. Boyer, C. Barner-Kowollik, Z. A. Page, *Matter* **2021**, *4*, 2172.

[2] a) A. Vitale, G. Trusiano, R. Bongiovanni, in *Progress in Adhesion and Adhesives*, (Ed: K. L. Mittal), John Wiley & Sons, Hoboken, USA **2018**, Vol. *3*, Ch. 4; b) Z. Liu, F. Yan, *Adv. Sci.* **2022**, *9*, 2200264.

[3] a) D. Habault, H. Zhang, Y. Zhao, *Chem. Soc. Rev.* **2013**, *42*, 7244; b) S. Wang, M. W. Urban, *Nat. Rev. Mater.* **2020**, *5*, 562.

[4] a) G. Delaittre, A. S. Goldmann, J. O. Mueller, C. Barner-Kowollik, *Angew. Chemie Int. Ed.* **2015**, *54*, 11388; b) J. del Barrio, C. Sánchez-Somolinos, *Adv. Opt. Mater.* **2019**, *7*, 1900598; c) D. Zhang, C. Li, G. Zhang, J. Tian, Z. Liu, *Acc. Chem. Res.* **2024**, *57*, 625.

[5] a) C. Barner-Kowollik, M. Bastmeyer, E. Blasco, G. Delaittre, P. Müller, B. Richter, M. Wegener, *Angew. Chem., Int. Ed.* **2017**, *56*, 15828; b) K. Jung, N. Corrigan, M. Ciftci, J. Xu, S. E. Seo, C. J. Hawker, C. Boyer, *Adv. Mater.* **2019**, *32*, 1903850; c) A. Bagheri, J. Jin, *ACS Appl. Polym. Mater.* **2019**, *1*, 593; d) S. C. Gauci, A. Vranic, E. Blasco, S. Bräse, M. Wegener, C. Barner-Kowollik, *Adv. Mater.* **2024**, *36*, 2306468.

[6] a) M. Regehly, Y. Garmshausen, M. Reuter, N. F. König, E. Israel, D. P. Kelly, C.-Y. Chou, K. Koch, B. Asfari, S. Hecht, *Nature* **2020**, *588*, 620; b) V. Hahn, P. Rietz, F. Hermann, P. Müller, C. Barner-Kowollik, T. Schlöder, W. Wenzel, E. Blasco, M. Wegener, *Nat. Photonics* **2022**, *16*, 784.

[7] a) N. Liaros, J. T. Fourkas, *Opt. Mater. Express* **2019**, *9*, 3006; b) M. He, Z. Zhang, C. Cao, G. Zhao, C. Kuang, X. Liu, *Laser Photonics Rev.* **2022**, *16*, 2100229.

[8] a) L. García-Fernández, C. Herbivo, V. S. M. Arranz, D. Warther, L. Donato, A. Specht, A. del Campo, *Adv. Mater.* **2014**, *26*, 5012; b) M. Kathan, P. Kovaříček, C. Jurissek, A. Senf, A. Dallmann, A. F. Thünemann, S. Hecht, *Angew. Chem., Int. Ed.* **2016**, *55*, 13882; c) J. T. Xu, S. Shanmugam, C. K. Fu, K. F. Aguey-Zinsou, C. Boyer, *J. Am. Chem. Soc.* **2016**, *138*, 3094; d) T. Krappitz, F. Feist, I. Lamparth, N. Moszner, H. John, J. P. Blinco, T. R. Dargaville, C. Barner-Kowollik, *Mater. Horiz.* **2019**, *6*, 81.

[9] a) N. D. Dolinski, Z. A. Page, E. B. Callaway, F. Eisenreich, R. V. Garcia, R. Chavez, D. P. Bothman, S. Hecht, F. W. Zok, C. J. Hawker, *Adv. Mater.* **2018**, *30*, 1800364; b) S. Bialas, L. Michalek, D. E. Marschner, T. Krappitz, M. Wegener, J. Blinco, E. Blasco, H. Frisch, C. Barner-Kowollik, *Adv. Mater.* **2019**, *31*, 1807288; c) L. Michalek, S. Bialas, S. L. Walden, F. R. Bloesser, H. Frisch, C. Barner-Kowollik, *Adv. Funct. Mater.* **2020**, *30*, 2005328; d) N. D. Dolinski, E. B. Callaway, C. S. Sample, L. F. Gockowski, R. Chavez, Z. A. Page, F. Eisenreich, S. Hecht, M. T. Valentine, F. W. Zok, C. J. Hawker, *ACS Appl. Mater. Interfaces* **2021**, *13*, 22065; e) K. C. H. Chin, G. Ovsepyan, A. J. Boydston, *Nat. Commun.* **2024**, *15*, 3867.

[10] a) Q. Ge, A. H. Sakhaei, H. Lee, C. K. Dunn, N. X. Fang, M. L. Dunn, *Sci. Rep.* **2016**, *6*, 31110; b) C. A. Spiegel, M. Hippler, A. Münchinger, M. Bastmeyer, C. Barner-Kowollik, M. Wegener, E. Blasco, *Adv. Funct. Mater.* **2020**, *30*, 1907615.

[11] a) K. Ehrmann, C. Barner-Kowollik, *J. Am. Chem. Soc.* **2023**, *145*, 24438; b) J. Hobich, E. Blasco, M. Wegener, H. Mutlu, C. Barner-Kowollik, *Macromol. Chem. Phys.* **2023**, *224*, 2200318.

[12] a) C. M. Sousa, J. R. Fernandes, P. J. Coelho, *Eur. Polym. J.* **2023**, *196*, 112312; b) L. Stüwe, M. Geiger, F. Röllgen, T. Heinze, M. Reuter, M. Wessling, S. Hecht, J. Linkhorst, *Adv. Mater.* **2024**, *36*, 2306716.

[13] a) S. L. Walden, L. L. Rodrigues, J. Alves, J. P. Blinco, V. X. Truong, C. Barner-Kowollik, *Nat. Commun.* **2022**, *13*, 2943; b) T. N. Eren, F. Feist, K. Ehrmann, C. Barner-Kowollik, *Angew. Chem., Int. Ed.* **2023**, *62*, 202307535.

[14] a) J. Fischer, G. Von Freymann, M. Wegener, *Adv. Mater.* **2010**, *22*, 3578; b) J. Fischer, M. Wegener, *Opt. Mater. Express* **2011**, *1*, 614; c) B. Harke, W. Dallari, G. Grancini, D. Fazzi, F. Brandi, A. Petrozza, A. Diaspro, *Adv. Mater.* **2013**, *25*, 904; d) R. Wollhofen, B. Buchegger, C. Eder, J. Jacak, J. Kreutzer, T. A. Klar, *Opt. Mater. Express* **2017**, *7*, 2538.

[15] a) T. Scott, B. Kowalski, A. Sullivan, C. Bowman, R. Mcleod, *Science* **2009**, *324*, 913; b) M. P. de Beer, H. L. van der Laan, M. A. Cole, R. J. Whelan, M. A. Burns, T. F. Scott, *Sci. Adv.* **2019**, *5*, eaau8723; c) A. Gruzdenko, D. J. Mulder, A. P. H. J. Schenning, J. M. J. denToonder, M. G. Debije, *ACS Appl. Mater. Interfaces* **2024**, *16*, 22696.

[16] a) P. Mueller, M. M. Zieger, B. Richter, A. S. Quick, J. Fischer, J. B. Mueller, L. Zhou, G. U. Nienhaus, M. Bastmeyer, C. Barner-Kowollik, M. Wegener, *ACS Nano* **2017**, *11*, 6396; b) H. Vijayamohanan, E. F. Palermo, C. K. Ullal, *Chem. Mater.* **2017**, *29*, 4754; c) P. Müller, R. Müller, L. Hammer, C. Barner-Kowollik, M. Wegener, E. Blasco, *Chem. Mater.* **2019**, *31*, 1966.

[17] M. Villabona, S. Wiedbrauk, F. Feist, G. Guirado, J. Hernando, C. Barner-Kowollik, *Org. Lett.* **2021**, *23*, 2405.

[18] F. Feist, J. P. Menzel, T. Weil, J. P. Blinco, C. Barner-Kowollik, *J. Am. Chem. Soc.* **2018**, *140*, 11848.

[19] Y. Gu, E. A. Alt, H. Wang, X. Li, P. Adam, J. A. Johnson, *Nature* **2018**, *560*, 65.

[20] a) A. Fihey, A. Perrier, W. R. Browne, D. Jacquemin, *Chem. Soc. Rev.* **2015**, *44*, 3719; b) A. Sherstiuk, M. Villabona, A. Lledós, J. Hernando, R. M. Sebastián, E. Hey-Hawkins, *Dalton Trans.* **2024**, *53*, 6190.